Rhizobacteria-induced systemic resilience in *Sorghum bicolor* (L.) moench against *Fusarium pseudograminearum* crown rot under drought stress conditions

René Carlson[a], Fidele Tugizimana[b], Paul A. Steenkamp[b], Ian A. Dubery[b],

Ahmed Idris Hassen[c] and Nico Labuschagne[a,*]

[a]Faculty of Natural and Agricultural Sciences, Department of Plant and Soil Sciences, University of Pretoria, Private Bag X20, Hatfield, Pretoria, 0028, South Africa

[b]Centre for Plant Metabolomics Research, Department of Biochemistry, Faculty of Science, University of Johannesburg, P.O. Box 524, Auckland Park, Johannesburg, SouthAfrica

[c]Agricultural Research Council, Plant Health and Protection, Private bag X134, Queenswood, Pretoria, 0121, South Africa

*Corresponding author.

E-mail addresses: renecarlson@gmail.com (R. Carlson), ftugizimana@uj.ac.za (F. Tugizimana), psteenkamp@uj.ac.za (P.A. Steenkamp), idubery@uj.ac.za (I.A. Dubery), HassenA@arc.agric.za (A.I. Hassen), nico.labuschagne@up.ac.za (N. Labuschagne)

Highlights

- *Fusarium pseudograminearum* crown rot and drought stress in sorghum was investigated.
- Seventy seven rhizobacterial isolates to induce systemic resilience were screened.
- Metabolomics revealed aspects of the mechanism of induced systemic resilience.
- Differential metabolic changes reflected biotic, abiotic and combined stresses.
- Synergistic effects and cross-talk are operative in induced systemic resilience.

Abstract

The potential of 77 rhizobacterial isolates to elicit induced systemic resilience (ISResilience) against combined biotic (*Fusarium pseudograminearum* crown rot) and abiotic (drought) stress in *Sorghum bicolor* was investigated. ISResilience was determined by assessing disease incidence and severity, plant height and biomass (root and shoots) in rhizobacteria-primed and untreated (naïve) plants inoculated with *F. pseudograminearum* and subjected to drought stress. Three rhizobacterial isolates (*Paenibacillus alvei* NAS-6G6, *Pseudomonas taiwanensis* N66 and *Bacillus velezensis* N54) showed significant protection of *S. bicolor* seedlings against biotic, abiotic and combined biotic and abiotic stress. Isolate N54, identified in this study as *B. velezensis* by 16S rRNA sequencing, was considered as the best performing rhizobacterial isolate to elicit ISResilience. Untargeted ultra-high performance liquid chromatography-high definition mass spectrometry (UHPLC-HDMS) based metabolomics was used to investigate the mechanism by which ISResilience was elicited in

S. bicolor by strain N54 (*B. velezensis*). Comparisons were made with isolates that were previously selected for induced systemic tolerance (ISTolerance) against drought stress (strain N66, *Ps. taiwanensis*) and induced systemic resistance (ISResistance) against *F. pseudograminearum* crown rot (strain NAS-6G6, *Pa. alvei*). The stress alleviation that resulted from treatment with the respective rhizobacterial isolates, was visually confirmed by the use of infrared (IR) thermography. For the metabolomics study, intracellular metabolites were methanol-extracted from rhizobacteria-primed and untreated (naïve) *S. bicolor* shoots. Extracts were analyzed on an UHPLC-HDMS platform, and the data were chemometrically analyzed to determine metabolite bio-markers related to ISResistance, ISTolerance and ISResilience. The results demonstrated significant treatment-related differences, reflecting differential metabolic reprogramming in *S. bicolor* in response to the biotic, abiotic and combined stresses. Synergistic effects involved in the lowered susceptibility to crown rot of rhizobacteria-primed *S. bicolor* seedlings, compared to those left naïve (untreated control) under drought stress conditions and the upregulation of the signatory molecules myo-inositol and riboflavin, provided evidence for the role of crosstalk in the ISResilience observed.

Abbreviations

BLAST - basic local alignment search tool
BPI - base peak intensity
CV-ANOVA - cross-validated analysis of variance
ESI - electrospray ionization
HCA - hierarchical clustering analysis
HD - high definition
ISResilience - induced systemic resilience
ISResistance - induced systemic resistance
IR - infrared
ISTolerance - induced systemic tolerance
LC - liquid chromatography
MOA - mode/s of action
MS - mass spectrometry
MSI - metabolomics standards initiative
NCBI - National Center for Biotechnology Information
NJ - neighbor joining
OPLS-DA - orthogonal partial least square-discriminant analysis
PCA - principal component analysis
PDA - potato dextrose agar
PGPR - plant growth-promoting rhizobacteria
QC - quality control
RbGU - rose bengal-glycerol-urea
RWC - relative water content
SA - salicylic acid
SAF - stress alleviation factor
UHP - ultra-high performance
VIP - variable importance in projection

Keywords: Drought; *Fusarium pseudograminearum* crown rot; Induced systemic resilience; PGPR; *Sorghum bicolor;* UHPLC-HDMS

1. Introduction

The interdependence between organisms and their environment is clearly illustrated in the classical disease triangle comprising pathogen, host and environment. Under changing climatic conditions plants will be subjected to biotic and abiotic stress factors more often, with more frequent stress interactions occurring (Kissoudis et al., 2014). Exploiting the functional diversity of beneficial microbes to mitigate biotic and abiotic stress, is considered to be the cornerstone of the next green revolution (Parnell et al., 2016). Research on the capacity of plant growth-promoting rhizobacteria (PGPR) to mitigate combined biotic and abiotic stress is limited, but it was shown to be of great potential to augment plant phenotypes, enabling more sustainable agriculture (Timmusk and Wagner, 1999, Lucas et al., 2014, Choudhary et al., 2016).

In addition to their plant growth-promoting properties, PGPR have also gained popularity for their capacity to mitigate environmental stress by inducing an enhanced defensive response in plants. This enhanced defense is the result of a PGPR-induced metabolic reprogramming that result in physical and/or chemical changes that augment the plant's innate defense response. PGPR are known to provide protection against biotic and abiotic stress. PGPR-induced resistance against biotic stress is known as induced systemic resistance (ISResistance; Harish et al., 2008, Walters, 2009, Walters and Fountaine, 2009), whereas PGPR-induced tolerance against abiotic stress is known as induced systemic tolerance (ISTolerance; Yang et al., 2009, Naseem and Bano, 2014, Ngumbi and Kloepper, 2016) and the enhanced resilience offered by PGPR against combined biotic and abiotic stress is known as induced systemic resilience (ISResilience; Timmusk and Wagner, 1999, Lucas et al., 2014, Choudhary et al., 2016).

The frequency of combined biotic and abiotic stress will increase in view of climate change projections. PGPR-induced physical and/or chemical changes in plants in response to combinations of abiotic and biotic stress, as a form of ISResilience, has thus received much attention lately (Timmusk and Wagner, 1999, Kissoudis et al., 2014, Lucas et al., 2014). Resilience is the capacity of a living organism to respond to a perturbation or disturbance by resisting damage and recovering quickly or the capacity to absorb shocks without losing structure and function. To date, studies have focused mainly on individually occurring biotic and abiotic stress. Although research in this area is of cardinal importance to elucidate the regulatory networks involved in plant defense response, research should also explore the combined effects of biotic and abiotic stress to ensure future food security (Koornneef et al., 2008).

The plant's response to combined biotic and abiotic stress is distinctly different to that of stress occurring individually (Fujita et al., 2006, Koornneef et al., 2008, Kissoudis et al., 2014). Regardless of this, the same basic regulatory networks are shared between the plant's biotic and abiotic stress responses, comprising of the production of nitric oxide and Ca^{2+} signaling in the early stages, followed by the production of stress signaling compounds that ultimately lead to the systemic production of stress proteins and metabolites. Although a great degree of overlap exists between the regulatory networks of the plant's biotic and abiotic stress responses, the effect of combined stress is usually non-additive and either antagonistic or synergistic (Pieterse, 2001, Pieterse et al., 2001, Fujita et al., 2006, Koornneef et al., 2008, Oktem et al., 2008, Moubayidin et al., 2009, Kissoudis et al., 2014, Yue et al., 2016, Rejeb et al., 2018). This supports the phenomenon of crosstalk and the convergence of regulatory pathways under combined biotic and abiotic stress (Kissoudis et al., 2014).

The differential metabolic reprogramming observed in PGPR-primed *Sorghum bicolor* systems during ISResistance and ISTolerance has been elucidated in earlier studies (Carlson et al., 2019, Tugizimana et al., 2019, Carlson et al., 2020). Under conditions of biotic stress, the differential metabolic reprogramming in rhizobacteria-primed *S. bicolor* plants comprised of a quicker and/or enhanced upregulation of amino acid-, phytohormone-, phenylpropanoid-, flavonoid- and lipid metabolites in response to inoculation with *F. pseudograminearum* (Carlson et al. 2019), whereas under conditions of abiotic stress the enhanced drought stress tolerance observed in rhizobacteria-primed *S. bicolor* plants included (1) augmented antioxidant capacity; (2) growth promotion and root architecture modification as a result of the upregulation of the hormones gibberellic acid, indole acetic acid and cytokinin; (3) the early activation of induce systemic tolerance through the signalling hormones brassinolides, salicylic acid and jasmonic acid and signalling molecules sphingosine and psychosine; (4) the production of the osmolytes proline, glutamic acid and choline; (5) the production of the epicuticular wax docosanoic acid and (6) ACC deaminase activity resulting in lowered ethylene levels (Carlson et al. 2020).

In this study a collection of 77 rhizobacterial isolates were screened for their potential to alleviate combined biotic (*F. pseudograminearum* crown rot) and abiotic (drought) stress in *S. bicolor* seedlings. The best-performing rhizobacterial isolate was identified using 16S rRNA gene sequencing techniques. An UHPLC-HDMS based metabolomics approach was used to investigate the effects of the best-performing isolate on the metabolome of *S. bicolor* seedlings in order to gather information that could potentially shed light on the modes of action (MOA) involved in rhizobacteria-induced resilience against combined biotic and abiotic stresses. A good understanding of the metabolic response of *S. bicolor* against individually occurring stress (Carlson et al., 2019, Carlson et al., 2020) provides a backdrop for the elucidation of the mechanisms involved in rhizobacteria-induced resilience against combined biotic and abiotic stress.

2. Materials and methods

2.1. Greenhouse screening of a collection of new rhizobacterial isolates for induced systemic resilience

2.1.1. Sorghum cultivation

Sorghum bicolor seed (cultivar Sweet NS 5655) was obtained from Advance Seed (Krugersdorp, South Africa). The seeds were sterilized successively in 70% ethanol (5 min), 1% sodium hypochlorite (1 min) and rinsed five times with sterile dH_2O. The seeds were subsequently transferred to Petri dishes containing filter paper moistened with sterile dH_2O and allowed to germinate for 48 h at 25 °C. The germinating seeds were inspected daily for any bacterial and fungal growth and contaminated seedlings were discarded. The *S. bicolor* germlings were directly planted into plastic seedling trays filled with washed, autoclaved (120 °C for 20 min), pure silica sand. The trays consisted of 30 cells of 50 mL capacity per tray and were sterilized with 10% sodium hypochlorite. The plants were watered every second day with sterilized dH_2O to field capacity and fertilized once a week with a general water-soluble fertilizer (Multifeed®, Nulandis, Kempton Park, South Africa). No pesticides or fungicides were needed. The greenhouse temperature was maintained at between 20 °C and 30 °C and the relative humidity fluctuated between 40% and 60%. At harvest, the fresh and dry weights of both roots and shoots were measured and samples for metabolomics analysis were taken (as described under 2.2.2.1). A total of three biological replicates were

included, consisting of 20 sorghum seedlings per replicate and thus 60 sorghum seedlings per treatment. Half of the harvested plant material (10 plants per replicate) was used for metabolomics analysis and the remaining half was used to assess disease incidence and severity.

2.1.2. Rhizobacterial inoculum preparation and application

The same collection of 77 rhizobacterial isolates, obtained from the University of Pretoria's PGPR collection as reported on in Carlson et al. (2020), were screened for their potential to induce systemic resilience against combined biotic stress (*F. pseudograminearum* crown rot) and abiotic stress (drought) in *S. bicolor* seedlings. The group of 77 isolates consisted of 74 new isolates (Hassen, 2007), 2 strains in the process of being commercialized by the University of Pretoria (*Paenibacillus alvei* NAS-6G6 and *Pa. alvei* T29) and 1 commercial strain (RhizoVital® *Bacillus amyloliquefaciens*, Andermatt Biocontrol AG, Switzerland). The bacterial isolates were maintained at −72 °C on Microbeads® (Davies diagnostics, Randburg, South Africa). The 74 isolates and 3 strains were streaked onto Nutrient agar and a 1 w old culture of each was inoculated into Nutrient broth and incubated in a rotary shaker at 25 °C and 150 rpm for 48 h. Each bacterial suspension was subsequently centrifuged in 50 mL capacity sterile plastic tubes at 2000 rpm for 10 min. The resulting pellet was re-suspended in quarter strength sterile Ringer's solution to give a final concentration of 10^8 cfu mL^{-1}. Three weeks after planting of the sorghum seed, each plant (one plant per pot) was treated with 1 mL of a 10^8 cfu mL^{-1} cell suspension of the respective rhizobacterial isolates/strains.

2.1.3. Implementation of biotic and abiotic stress

2.1.3.1. Biotic stress

The crown rot pathogen *F. pseudograminearum* (strain M7816N) was obtained from Dr. Sandra Lamprecht at the Agricultural Research Council, Plant Health and Plant Protection Research Institute (Stellenbosch, South Africa). In order to retain virulence the strain was aseptically stored on filter paper discs in McCartney bottles at 5 °C (Fong et al., 2000). When needed, one disc was aseptically removed from the McCartney bottle and plated onto half strength potato dextrose agar (PDA). Five 5 mm diameter discs were subsequently taken from the edge of a 72 h PDA culture and inoculated into 500 mL mungbean liquor medium (Bai and Shaner, 1996). A final spore suspension at a concentration of 1×10^6 mL^{-1}, determined using a counting chamber, was used for inoculation (Akinsanmi et al., 2004, Xi et al., 2008). A wetting agent (Tween 20) was added to the spore suspension at 0.1% v/v. Twenty one days after seeding of pre-germinated *S. bicolor* seed, a small piece (30 × 15 mm) of sterilized absorbent cotton wool was wrapped around the base of the stem, 1 cm above the soil level, and held in place by masking tape (15 mm wide). Plants were inoculated by pipetting 500 µL of the conidial suspension onto the cotton wool in a similar fashion as described by Carlson et al., 2019, Mitter et al., 2006. Control treatments received 500 µL of pathogen-free mungbean liquor medium.

2.1.3.2. Abiotic stress

Four days after priming plants with each rhizobacterial isolate (coinciding with three days post inoculation with the pathogen), *S. bicolor* seedlings were subjected to drought stress once weekly for a period of 3 w. Plants were monitored hourly, until sufficient wilting was

observed in the non-rhizobacteria-amended control plants. At this point all cells were watered to field capacity. The unstressed control plants were not subjected to drought stress.

2.1.4. Assessment of resilience against biotic and abiotic stress

At 6 w post planting, *S. bicolor* plants were assessed for ISResilience. Plant heights were recorded just before harvest. The plants were then removed by watering each pot to field capacity with tap water to loosen the roots in order to avoid breakage. The roots were then washed to remove any remaining sand particles and blotted dry with tissue paper. The biomass of both roots and shoots, percentage diseased plants (disease incidence) and lesion severity (disease severity; Li et al., 2008) were recorded. Furthermore, isolations were made from the crown area of the sorghum seedlings. Excised, surface-sterilized stem segments were plated onto rose bengal-glycerol-urea (RbGU) medium (Van Wyk and Scholtz, 1995) and those stem segments that yielded growth on the *Fusarium*-selective medium were recorded. Fresh weights were taken directly after harvest, whereas dry weights were taken after the plant material was dried in an oven at 40 °C for 48 h.

2.1.5. Statistical analyses

Data were subjected to analysis of variance and means were compared using Tukey's least significant difference (LSD) test at a significance level of $p < 0.05$. A total of three biological replicates were included.

2.1.6. Stress alleviation factor

Based on the results of the various rhizobacterial treatments, the individual rhizobacterial isolates were scored according to their ability to induce systemic resilience against combined biotic stress (*F. pseudograminearum* crown rot) and abiotic stress (drought) in *S. bicolor* plants. This was done by calculating a stress alleviation factor (SAF) incorporating the percentage increase in plant growth (plant height, root biomass, shoot biomass) and the percentage reduction in disease parameters (disease incidence, severity and isolations) as described in section 2.1.3. The SAF for ISResilience was formulated for the current study and calculated for each rhizobacterial isolate according to the equation:

$$\text{SAF\_ISResilience} = \frac{\left(\frac{Ih-Ch}{Ch}\times 100\right)+\left(\frac{Ir-Cr}{Cr}\times 100\right)+\left(\frac{Is-Cs}{Cs}\times 100\right)+\left(\frac{Cdi-Idi}{Cdi}\times 100\right)+\left(\frac{Cds-Ids}{Cds}\times 100\right)+\left(\frac{Cdl-Idl}{Cdl}\times 100\right)}{6}$$

where: *I* = isolate; *C* = untreated stress control; *h* = plant height; *r* = root dry biomass; *s* = shoot dry biomass; *di* = disease incidence; *ds* = disease severity; *dl* = disease isolations.

2.1.7. Identification of best-performing rhizobacterial isolate using 16S rRNA gene sequence analysis

Genomic DNA was extracted from the best-performing rhizobacterial isolate using a Promega Wizard genomic DNA purification kit (Promega Corporation, USA) following manufacturer's instructions. The 16S ribosomal RNA region was amplified by the polymerase chain reaction (PCR) using primers 27F (5′-AGA GTT TGA TCM TGG CTC AG-3′) corresponding to *E. coli* numbering 8–27 (Lane, 1991) and 1485R (5′-TAC GGT

TAC CTT GTT ACG AC-3′) corresponding to *E. coli* numbering 1489–1508 (Embley et al., 1988). The PCR was performed with OneTaq Quick-Load 2X Master Mix containing 1 × standard PCR buffer, 1.8 mM $MgCl_2$, 0.5 μM of each primer, 0.2 μM of each dNTP, 0.3 U OneTaq® DNA Polymerase (New England Biolabs, USA). To obtain the 16S rRNA (27F/1485R) amplicons, 35 × PCR cycles were performed that include initial denaturation at 94 °C for 3 min, denaturation at 94 °C for 1 min, annealing at 56 °C for 1 min, extension at 72 °C for 1 min and second extension at 72 °C for 5 min. The PCR product was separated by electrophoresis through 1% agarose gel, purified and sequenced (Inqaba Biotechnical Industries, Pretoria, South Africa). The resulting sequence was edited on BioEdit program version 7 (http://www.mbio.ncsu.edu/BioEdit/bioedit.html) after which it was aligned using the Clustal W alignment tool. The MEGA 7 software was used to construct maximum likelihood phylogenetic trees based on bootstrap analysis of 1000 replicates to calculate the statistical significance of the branches of the phylogenetic tree (Kumar et al., 2018). The nucleotide sequence of the 16S rRNA was deposited in the GenBank at the National Center for Biotechnology Information (NCBI, https://www-ncbi-nlm-nih-gov.uplib.idm.oclc.org/WebSub/) with accession number MK855501.

2.2. Metabolomics study

2.2.1. Assessment of induced systemic resilience

Three rhizobacterial isolates that offered significant protection against (1) biotic stress (*Pa. alvei* NAS-6G6: protection against *F. pseudograminearum* crown rot; Carlson et al., 2019), (2) abiotic stress (*Ps. taiwanensis* strain N66: protection against drought stress; Carlson et al., 2020) and (3) a combination of both biotic and abiotic stress (isolate N54: protection against both biotic and abiotic stress) were included as treatments. A total of three biological replicates were included, consisting of 20 sorghum seedlings per replicate and thus 60 sorghum seedlings per treatment. Half of the harvested plant material (10 plants per replicate) was used for metabolomics analysis and the other half for assessment of disease incidence and isolations made from crown rot lesions.

2.2.1.1. Preparation and application of rhizobacterial isolates and amendment method

The rhizobacterial isolates were maintained at −72 °C on Microbeads® (Davies diagnostics, Randburg, South Africa). Each isolate was prepared as detailed under section 2.1.2. Three weeks after planting, 1 mL of a 10^8 cfu mL^{-1} rhizobacterial cell suspension, in quarter strength sterile Ringer's solution, was applied to each cell in the seedling tray.

2.2.1.2. Inoculation with the fungal pathogen

The same *F. pseudograminearum* strain mentioned under section 2.1.3.1. was used. Pathogen maintenance, inoculum preparation and inoculation were done as outlined above under section 2.1.3.1.

2.2.1.3. Implementation of drought stress

Four days after treatment (priming) of the plants with each of the three selected rhizobacterial isolates, the *S. bicolor* seedlings were subjected to drought stress (once only). Plants were monitored hourly until sufficient wilting was noticed in non-rhizobacteria-treated (naïve) plants at which point all pots were watered to field capacity with sterilized dH_2O. The non-

stressed control plants were not subjected to drought stress. Samples for metabolomics analysis were taken 24 h post drought stress.

2.2.1.4. Assessments

At 6 w post planting a biotic and abiotic stress assessment was done by means of IR thermography, relative water content (RWC), measurement of plant height, root length and plant biomass (roots and shoots) and assessment of disease incidence. The RWC was calculated as outlined by Seelig et al. (2008), the only exception being that dry weight was obtained after oven-drying samples at 40 °C for 48 h. Disease incidence was calculated as the percentage plants with crown rot lesions out of the total number of plants assessed. Furthermore, isolations were made from the crown area of the sorghum seedlings. Excised, surface-sterilized stem segments were plated onto rose bengal-glycerol-urea (RbGU) medium (Van Wyk and Scholtz, 1995) and the segments that yielded fungal growth on the *Fusarium*-selective medium were recorded. IR thermography measurements of the leaf temperatures were made using a FLIR thermal imager (Testo 869 Thermal Imaging Camera, RS Components, UK). The data were subjected to analysis of variance and means were compared using Tukey's LSD test at a significance level of $p < 0.05$. A total of three biological replicates were included.

2.2.2. Ultra-high performance liquid chromatography-high definition mass spectrometry

Samples for UHPLC-HDMS were collected at 24 h post drought stress from stressed and non-stressed *S. bicolor* shoots of which each group was primed with each rhizobacterial strain/isolate or left naïve (untreated control).

2.2.2.1. Sample collection

Fresh leaf samples for UHPLC-HDMS analysis were taken 24 h post drought stress, which coincided with 5 d post treatment with each of the best-performing rhizobacterial isolates. The leaf samples were collected from drought stressed and non-stressed *S. bicolor* plants of which each group was primed with each of the rhizobacterial isolates or left naïve (untreated control). Leaves were weighed and then placed in a 50 mL centrifuge tube, instantly flash-frozen with liquid nitrogen and kept at −72 °C until time of metabolite extraction. Immediately before extraction, each frozen leaf sample was crushed to a powder by making use of a clean spatula. During the crushing process, each sample was kept frozen by adding liquid nitrogen as needed. One gram of the crushed sample was then transferred to a 50 mL centrifuge tube. The extraction process followed immediately thereafter making sure that the sample remained frozen up to this point.

2.2.2.2. Metabolite extraction

Intracellular metabolites were extracted with 80% methanol [1:10 (w/v)]. The 80% methanol mixture was homogenized using an Ultra Turrax homogenizer. The samples were subsequently centrifuged for 20 min at 5100 rpm at 4 °C. Supernatants were removed and evaporated under vacuum by using a rotary evaporator at 55 °C to a final volume of approximately 1 mL and transferred to Eppendorf tubes where it was dried in a vacuum centrifuge at 40 °C for 6 h to complete dryness. The dried samples were subsequently resuspended to a final volume of 500 µL (50:50, MeOH:MilliQ water) and filtered through 0.22 µm nylon syringe filters (Anatech, Randburg, South Africa) into HPLC glass vials fitted

with 500 µL inserts and stored at −20 °C. For quality control (QC) purposes, pooled samples were prepared by pipetting and mixing aliquots of equal volume from all samples.

2.2.2.3. Ultra-high performance liquid chromatography-high definition mass spectrometry analysis

The methanolic extracts were analyzed on a Waters Acquity UHPLC coupled in tandem to a Waters SYNAPT G1 Q-TOF mass spectrometer (Waters Corporation Milford, USA). The batch consisted of a total of 48 samples comprising 16 treatments [rhizobacterial treatment (4) *vs.* stress (4)], 3 biological replicates and each sample was injected 3 times (a total of 144 injections) to account for any technical variability. Chromatographic separation was attained using a Waters Acquity HSS T3 C18 column (150 mm × 2.1 mm × 1.8 µm) thermostatted at 60 °C. The T3 column is a reversed phase C18 column with optimised ligand density to reduce hydrophobisity, thus enabling the separation of both polar- and non-polar compounds. A binary solvent system consisting of 0.1% aqueous formic acid (Sigma-Aldrich, Munich, Germany) (solvent A) and 0.1% formic acid in acetonitrile (Romil Pure Chemistry, Cambridge, UK) (solvent B) was used, with a gradient elution at a flow rate of 0.4 mL min^{-1}. The initial conditions of 98% A and 2% B were held for 1 min followed by 30% A and 70% B at 14 min. At 15 min the conditions were changed to 5% A and 95% B, these conditions were held for 2 min and then changed to the initial conditions. The analytical column was allowed to equilibrate for 2 min before the next injection. The total chromatographic run time was 20 min and the injection volume was 2 µL. For the MS analyses, data were acquired in both positive and negative electrospray ionization (ESI) modes; and the MS conditions were set as follows: capillary voltage of 2.5 kV, sampling cone at 30 V, extraction cone at 4 V, cone gas flow 50 L h^{-1}, desolvation gas flow 550 L h^{-1}, source temperature at 120 °C, desolvation temperature at 450 °C, scan time of 0.1 s and mass range of 100–1000 Da. Leucine encephalin (50 pg mL^{-1}) was used as a calibrant to acquire mass accuracies between 1 and 3 mDa and data were acquired at different collision energies (MS^E, 10–50 eV) to aid with structural elucidation and annotation of the analytes. The sample acquisition was done in a randomized order. For quality assurance and control, solvent blanks (to monitor background noise from the solvent) and the QC samples were included in the batch. For QC samples, six QC injections were done at the beginning of the batch, and six QC injections were placed after every 30 sample injections in the QC sample (6 injections).

2.2.2.4. Data analysis

The datasets were processed using Markerlynx XS™ software (Waters Corporation, Milford, USA). Alignment, peak finding, peak integration and retention time (Rt) correction were done on a Rt range of 1.5–15 min, *m*/*z* range of 100–1000 Da, mass tolerance of 0.05 Da and Rt window of 0.2 min. Data were normalized to total intensity using Markerlynx XS. The datasets were exported to the SIMCA (soft independent modelling of class analogy) software version 14 (Umetrics, Umea, Sweden) for data pre-treatment and multivariate data analyses (MVDA) including principal component analysis (PCA), hierarchical clustering analysis (HCA) and orthogonal partial least square-discriminant analysis (OPLS-DA). Before computing these MVDA models, data were mean centered and Pareto-scaled. The computed and used models were validated as described in the results section.

2.2.2.5. Metabolite annotation

The annotation of metabolites were performed using Taverna workbench for PUTMEDID_LCMS Metabolite ID Workflows (Brown et al., 2009, Brown et al., 2011) that allows for the integrated, automated and high-throughput annotation and putative identification of metabolites from liquid chromatography-electrospray ionization-mass spectrometry (LC-ESI-MS) metabolomic data. The workflows consist of correlation analysis, metabolic feature annotation and metabolite annotation. The MarkerLynx-based data matrix was first formatted to match the Taverna workbench requirements. Three main workflows formed the Taverna metabolite identification procedure: (i) A Pearson-based correlation analysis (List_CorrData) was used to calculate rank correlations, (ii) metabolic feature annotation (annotate_Massmatch) that uses this correlation coefficient information for correlation analysis to allow the grouping of ion peaks with similar features such as Rt, and annotating features with the type of *m*/*z* ion (molecular ion, isotope, adduct, others) believed to originate from the same compound. The elemental composition / molecular formula (MF) of each *m*/*z* ion was then automatically calculated; and (iii) metabolite annotation (matchMF-MF) of the calculated MF (from the output file from workflow 2) was automatically compared and matched to the MF from a pre-defined reference file of metabolites (inhouse library). Metabolite annotation was confirmed by the following steps: (i) the MF of a selected metabolite candidate was manually searched on bioinformatics tools and database, such as SorghumbicolorCyc (https://www.plantcyc.org/databases/sorghumbicolorcyc/5.0), KEGG (Kyoto Encyclopedia of Genes and Genomes, www.genome.jp/kegg/) and Chemspider (www.chemspider.com), and (ii) structural confirmation through careful inspection of fragmentation patterns by examining the MS^1 and MS^E spectra of the selected metabolite candidate; (iii) comparative assessment with/against annotation details of metabolites in *S. bicolor*, reported in literature, particularly in Dykes and Rooney (2006) and Kang et al. (2015). Metabolites were annotated to level 2 as classified by the Metabolomics Standard Initiative (MSI) (Sumner et al., 2007).

2.2.2.6. Metabolic pathway analysis

The MetaboAnalyst bioinformatics tool suite (version 3.0; http://www.metaboanalyst.ca/) was used to perform metabolomics pathway analysis (MetPA). The input into MetPA tool were the annotated metabolites from the OPLS-DA models. MetPA is a dedicated web-based pathway analysis and visualization tool that comprises several pathway enrichment analysis methods and the analysis pathway topological characteristics to enable the elucidation of most relevant and altered pathways involved in the conditions under consideration (Xia et al., 2015).

3. Results

3.1. Greenhouse screening of a collection of new rhizobacterial isolates for induced systemic resilience

Seventy-seven rhizobacterial isolates were screened for their potential to trigger ISResilience in *S. bicolor* seedlings against *F. pseudograminearum* crown rot under drought stress conditions. The ISResilience potential of each isolate was determined by assessing six parameters namely plant height, plant biomass (roots and shoots) and disease incidence and severity. Furthermore, isolations were made from the crown area of the sorghum seedlings. Excised, surface- sterilized stem segments were plated onto RbGU medium (Van Wyk and

Scholtz, 1995) and those isolations that yielded growth on the Fusarium-selective medium were recorded. A stress alleviation factor (SAF_ISResilience) was calculated from these parameters for each isolate, as outlined under materials and methods (section 2.1.6), and the results are given under supplementary material in Table S1.

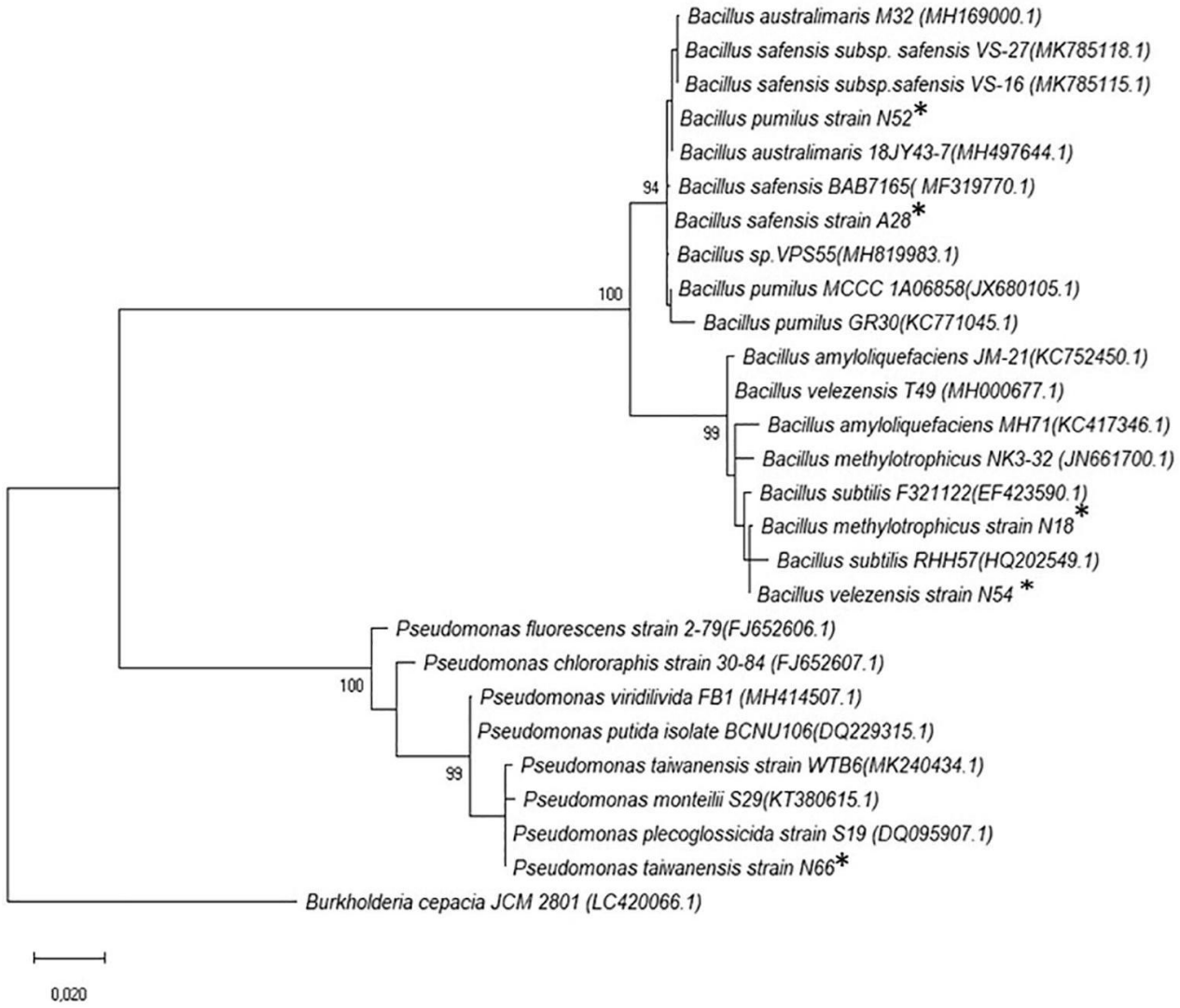

Fig. 1. Phylogenetic relatedness of the rhizobacterial isolates selected for ISTolerance: *Bacillus methylotrophicus* N18; *Bacillus safensis* A28; *Bacillus pumilus* N52 and *Pseudomonas taiwanensis* N66 (indicated with an asterisk; Carlson et al., 2020) and ISResilience: *Bacillus velezensis* N54 (indicated with an asterisk) in *S. bicolor* seedlings. Twenty two reference isolates were included in the phylogenetic tree to aid in identification. The evolutionary history was inferred using the Neighbor-Joining method (Saitou and Nei, 1987). The optimal tree with the sum of branch length = 0.65642332 is shown. The tree is drawn to scale, with branch lengths in the same units as those of the evolutionary distances used to infer the phylogenetic tree. The evolutionary distances were computed using the Maximum Composite Likelihood method (Tamura et al., 2004) and are in the units of the number of base substitutions per site. This analysis involved 9 nucleotide sequences. Codon positions included were 1st + 2nd + 3rd + Noncoding. All ambiguous positions were removed for each sequence pair (pairwise deletion option). There were a total of 1565 positions in the final dataset. Evolutionary analyses were conducted in MEGA.

The best-performing rhizobacterial isolate N54 was selected based on its performance in protecting *S. bicolor* against *F. pseudograminearum* under drought stress conditions, as indicated by its SAF_ISResilience (Table S1). The 16S rRNA sequence of this isolate was edited and BLAST searched on NCBI nucleotide database (BLASTN, Zhang et al., 2000), which resulted in 100% similarity with *Bacillus velezensis*. A phylogenetic tree was constructed using the neighbor joining (NJ) algorithm to compare its taxonomic relatedness with 20 reference strains together with those chosen as best-performing rhizobacterial isolates for ISTolerance (Carlson et al., 2020) and ISResistance (Carlson et al., 2019; Fig. 1). The analysis finally resulted in the identification of rhizobacterial isolate N54 as *B. velezensis*.

3.2. Metabolomics study

3.2.1. Comparing the best-performing PGPR isolates for their ability to elicit ISResistance, ISTolerance and ISResilience in S. bicolor seedlings.

The results of the assessment of the best-performing rhizobacterial isolates for elicitation of ISResistance, ISTolerance and ISResilience in *S. bicolor* seedlings are presented in Table 1. The corresponding IR thermography images of the untreated stress control treatments (naïve plants) are given in the supplementary material in Fig. S1, showing only the effects of all the stress regime combinations on *S. bicolor* seedlings. Treatment effects were statistically significant ($p < 0.05$) for all parameters assessed, except for RWC. All the stress treatments (separate and combined effects), significantly increased average leaf temperatures and disease incidence whilst lowering plant biomass (roots and shoots). Crown rot disease incidence and percentage isolations yielding *F. pseudograminearum* were elevated under drought stress conditions. All three the rhizobacterial isolates (*Pa. alvei* NAS-6G6, *Ps. taiwanensis* N66 and *B. velezensis* N54) reduced the effects of drought stress, crown rot incidence and combined (biotic and abiotic) stress to some extent, by lowering average disease incidence and increasing plant biomass (roots and shoots).

3.2.2. Metabolic profiling

Visual inspection of the base peak intensity (BPI) UHPLC-HDMS chromatograms [examples of electrospray ionization (ESI)-positive data for *S. bicolor* shoots are shown in Fig. 2], evidently showed differential peak populations (presence, intensities) in naïve *S. bicolor* seedlings under biotic (inoculation with *F. pseudograminearum*), abiotic (drought) and combined stresses *versus* those primed with *B. velezensis* N54 (chosen for its ISResilience activity) under combined biotic and abiotic stress conditions, reflecting differential metabolite profiles and composition. Thus, in order to elucidate informative description of specific metabolic features related to the observed differential chromatographic profiles, data mining and comparative chemometric analyses were performed as described under the experimental section. Chemometric analyses employed included unsupervised methods, such as principal component analysis (PCA), hierarchical clustering analysis (HCA) (an example of the ESI-positive data is shown in Fig. 3) and a supervised approach, namely orthogonal partial least square-discriminant analysis (OPLS-DA, an example of the ESI-positive data is shown in Fig. 4). The PCA and HCA (Fig. 3) provide an unsupervised overview of the ESI-positive data. The close clustering of the quality control (QC) samples in the PCA scores plot, indicate that the LC-MS system was stable and the results reproducible. The PCA model explains 68.0% variation in the Pareto-scaled data ($R^2X = 0.680$) and 48.1% predicted variation according to cross-validation ($Q^2 = 0.481$). The HCA dendrograms supported the treatment-related clustering/groupings observed in the PCA.

Table 1. Effect of the best-performing rhizobacterial isolates on *S. bicolor* seedlings subjected to each of the rhizobacterial isolates for ISResistance (*Paenibacillus alvei* NAS-6G6), ISTolerance (*Pseudomonas taiwanensis* N66) and ISResilience (*Bacillus velezensis* N54) under biotic abiotic and combined stresses.

Rhizobacteria		Pathogen	Stress	Biomass [1]				Crown rot [1]				RWC 1, 2		IR thermography (°C) [3]			
Isolate	Dosage (cfu/plant)	Dosage (spores/plant)		Shoots (g)		Roots (g)		Incidence (%)		Isolations (%)		(%)		Leaf average 1, 4		Min. [5]	Max. [6]
None	–	None	None	1.59	ab	1.37	a	0.00	d	0.00	e	97.5	a	22.3	d	20.80	26.90
None	–	1×10^6	None	1.59	ab	1.44	a	50.00	b	41.67	bc	105.8	a	20.4	e	19.20	25.30
None	–	None	Drought	0.96	g	0.92	ab	0.00	d	0.00	e	63.8	a	24.6	a	20.40	33.00
None	–	1×10^6	Drought	0.97	fg	0.77	ab	87.50	a	100.00	a	104.2	a	23.7	bc	20.50	32.10
NAS-6G6	1×10^8	None	None	1.43	bc	1.03	ab	0.00	d	0.00	e	113.1	a	–		–	–
NAS-6G6	1×10^8	1×10^6	None	1.64	a	1.42	bc	20.83	cd	21.43	d	80.10	a	20.2	e	19.60	25.80
NAS-6G6	1×10^8	None	Drought	1.16	ef	1.13	bcd	0.00	d	0.00	e	81.6	a	–		–	–
NAS-6G6	1×10^8	1×10^6	Drought	1.16	ef	1.02	cd	29.17	bc	49.40	b	84.7	a	–		–	–
N66	1×10^8	None	None	1.41	bcd	1.29	abc	0.00	d	0.00	e	107.9	a	–		–	–
N66	1×10^8	1×10^6	None	1.60	ab	1.34	ab	33.33	bc	26.19	bcd	75.80	a	–		–	–
N66	1×10^8	None	Drought	1.00	fg	0.75	f	0.00	d	0.00	e	60.4	a	22.8	cd	19.90	31.80
N66	1×10^8	1×10^6	Drought	1.13	efg	0.91	def	50.00	b	100.00	a	92.4	a	–		–	–
N54	1×10^8	None	None	1.66	a	1.41	a	0.00	d	0.00	e	99.2	a	–		–	–
N54	1×10^8	1×10^6	None	1.37	cd	0.93	def	22.22	c	25.00	cd	81.9	a	–		–	–
N54	1×10^8	None	Drought	1.22	de	0.99	def	0.00	d	0.00	e	57.8	a	–		–	–
N54	1×10^8	1×10^6	Drought	1.13	efg	1.04	cd	45.83	b	37.50	bcd	60.0	a	23.7	b	20.30	31.40

[1]Means within columns followed by the same letter does not differ significantly according to Tukey's LSD test at a significance level of $p < 0.05$.
[2]Relative water content (RWC) was calculated as described by Seelig et al., (2008, section 2.2.1.5).
[3]IR thermography measurements of the leaf temperatures were made using a FLIR thermal imager (Testo 869 Thermal Imaging Camera, RS Components, UK) as shown in Fig. S1.
[4]Average temperature of 10 leaves per treatment measured using a FLIR thermal imager.
[5]Minimum temperature recorded for the entire seedling tray (consisting of 30 cells/plants) per treatment, measured using a FLIR thermal imager as shown in Fig. S1.
[6]Maximum temperature recorded for the entire seedling tray (consisting of 30 cells/plants) per treatment, measured using a FLIR thermal imager as shown in Fig. S1.

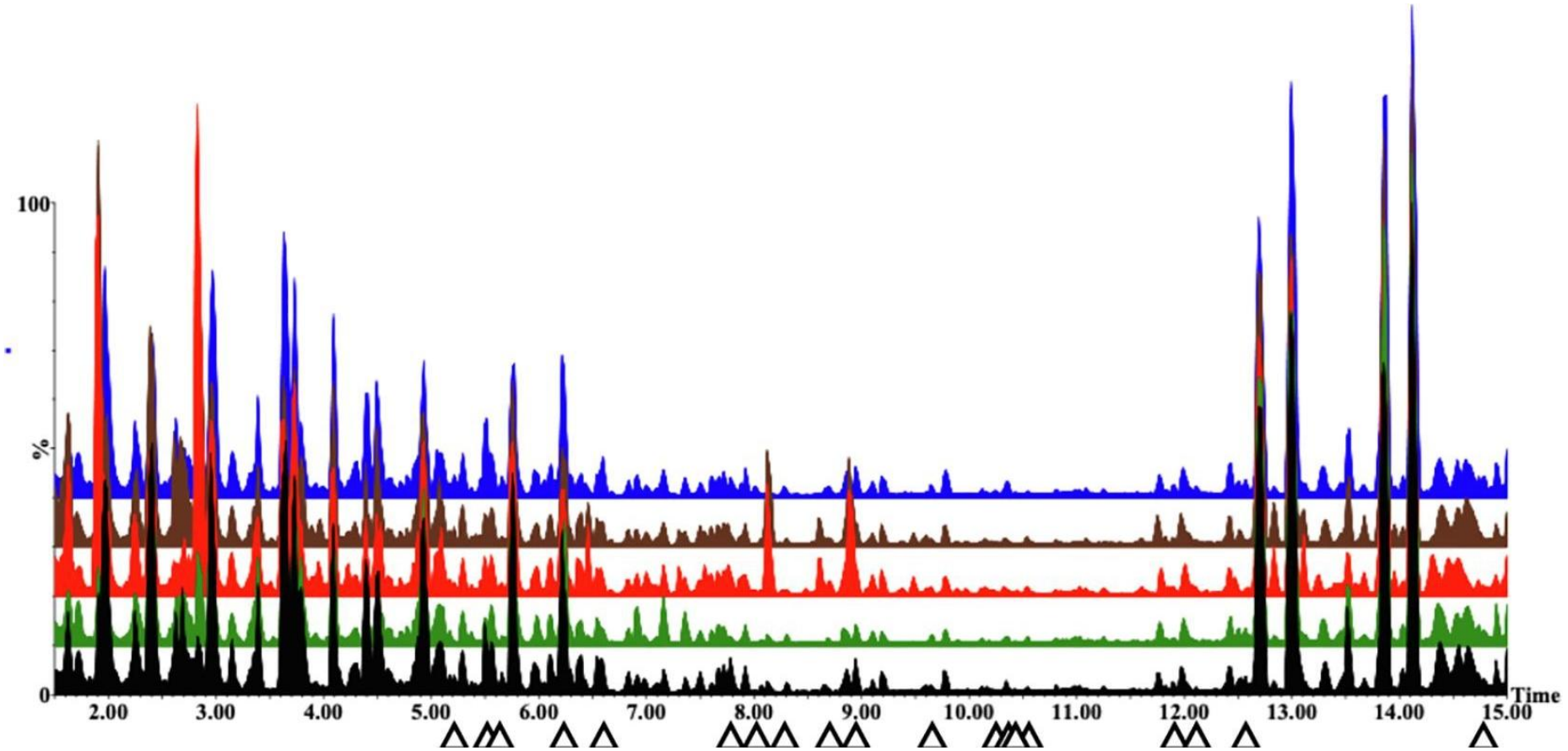

Fig. 2. UHPLC-HDMS BPI chromatograms of ESI-positive data obtained from *S. bicolor* shoots, indicating the metabolomic profiles of treatments (from bottom to top): (1) untreated control receiving no stress (black); (2) untreated control + biotic stress (*F. pseudograminearum* inoculation) (green); (3) untreated control + abiotic stress (drought) (red); (4) untreated control + combined biotic and abiotic stress (brown) and (5) amendment with N54 + combined biotic and abiotic stress (blue). The triangles below the x-axis indicate the peaks of features that were upregulated in N54-primed *S. bicolor* shoots (blue) *vs.* those left naïve (brown) under conditions of biotic (*F. pseudograminearum* inoculation) and abiotic (drought) stress.

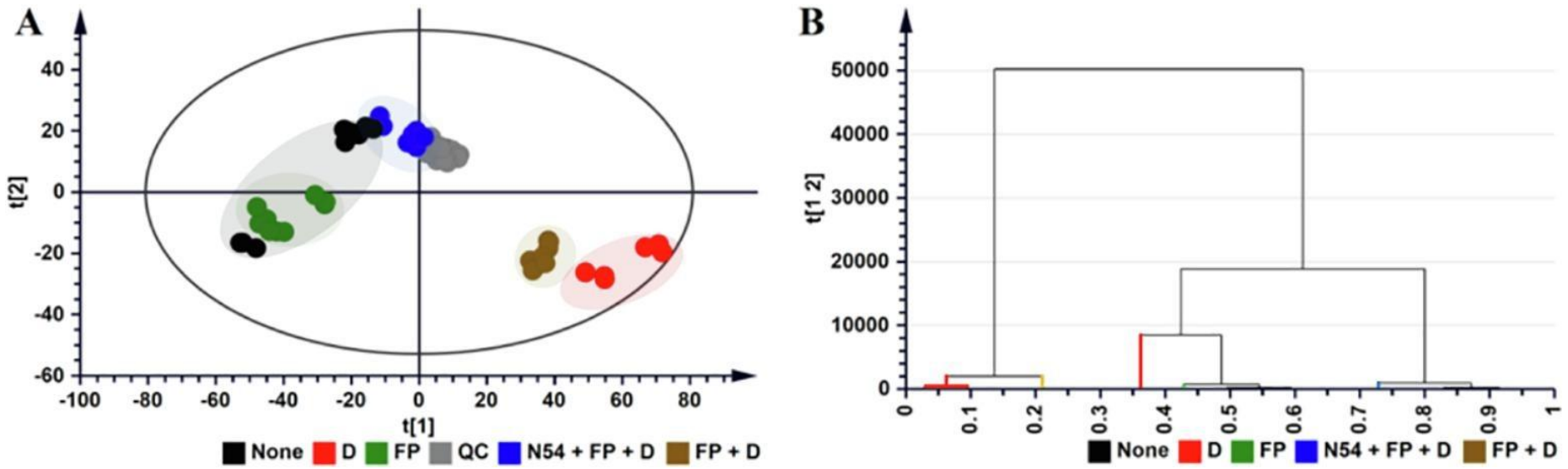

Fig. 3. Unsupervised chemometric overview of ESI-positive data obtained from *S. bicolor* shoots. (A) PCA score scatter plot computed from the first two PCs of an 6-component PCA model. The model explains 68.0% variation in the Pareto-scaled data ($R^2X = 0.680$) and 48.1% predicted variation according to cross-validation ($Q^2 = 0.481$). (B) HCA dendrogram corresponding to (A). Legend: None: amendment with N54 + no stress (black); D: untreated control subjected to drought stress (red); FP: untreated control inoculated with *F. pseudograminearum* (green); QC: Quality control samples (grey); N54 + FP + D: primed with N54, inoculated with *F. pseudograminearum* and subjected to drought stress (blue); FP + D: untreated control inoculated with *F. pseudograminearum* and subjected to drought stress.

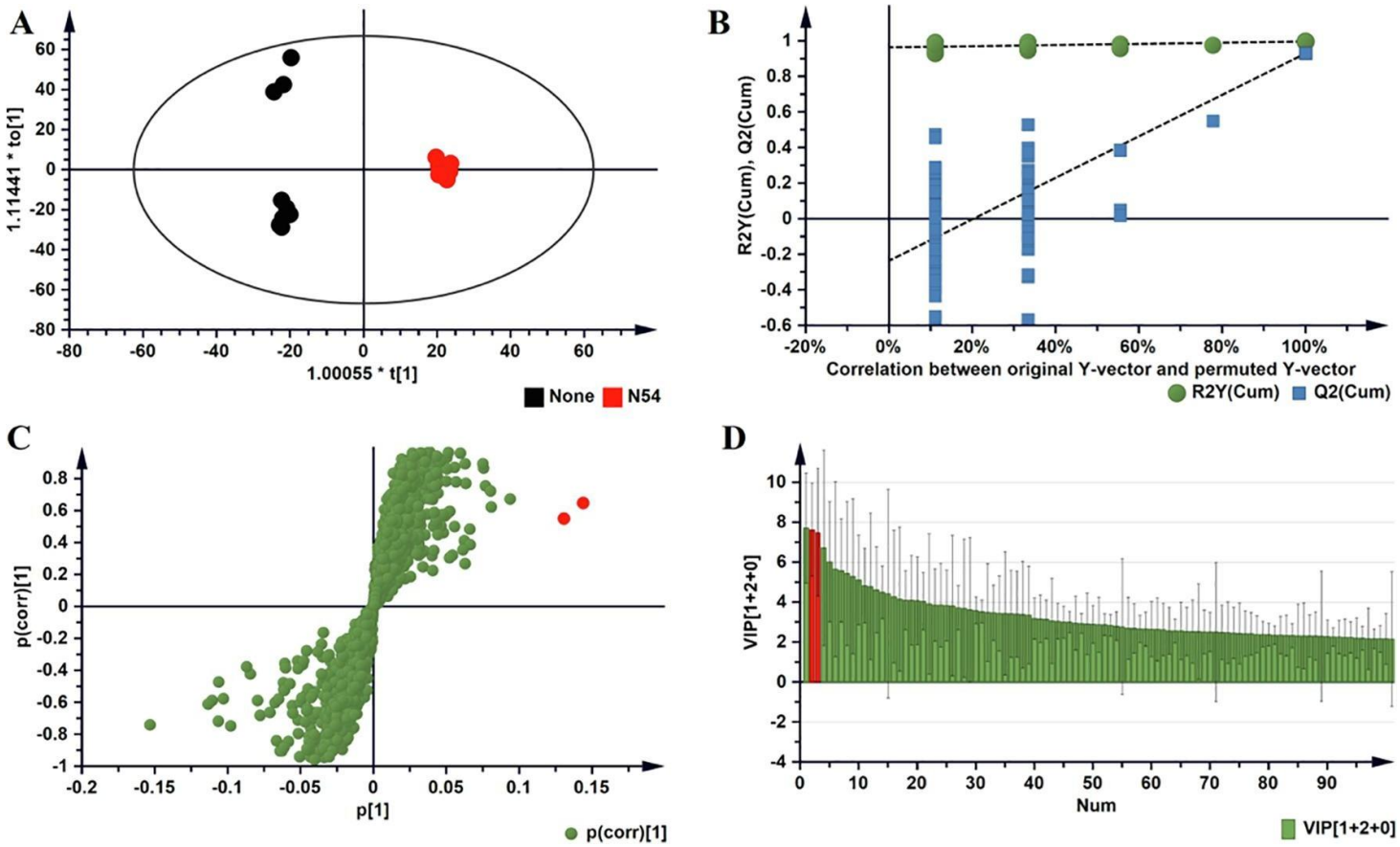

Fig. 4. OPLS-DA modelling of *S. bicolor* shoots samples and variable/feature selection of UHPLC-HDMS (ESI-positive) data. (A) A typical scores scatter plot for the OPLS-DA model separating *F. pseudograminearum*-inoculated and drought stressed plants that were (1) left untreated (None) *vs.* (2) N54-treated (N54) (1 + 2 + 0 components, $R^2X = 0.479$, $Q^2 = 0.929$, CV-ANOVA $p < 0.05$). In the scores plot, it is evident that the two groups are clearly separated: None *vs.* N54. (B) A typical response permutation test plot (n = 100) for the OPLS-DA model in (A); the R^2 and Q^2 values of the permutated models correspond to *y*-axis intercepts: $R^2 = (0.0, 0.988)$ and $Q^2 = (0.0, -0.295)$; (C) An OPLS-DA loadings S-plot for the same model in (A); variables situated in the extreme end of the S-plot are statistically relevant and represent prime candidates as discriminating variables/features. (D) A variable importance for the projection (VIP) plot for the same model; pointing mathematically to the importance of each variable (feature) in contributing to group separation in the OPLS-DA model.

Pa. alvei NAS-6G6, selected for its ISResistance activity (Carlson et al., 2019) and *Ps. taiwanensis* N66, selected for its ISTolerance activity (Carlson et al., 2020) were subjected to the same supervised and unsupervised chemometric analyses as described here for *B. velezensis* N54. An example of the unsupervised chemometric analysis of the ESI-positive data of the combined effects of all four stress regimes (no-stress, inoculation with *F. pseudograminearum*, subjection to drought stress and combined stresses) and rhizobacterial-treatments (untreated control, *Pa. alvei* NAS-6G6, *Ps. taiwanensis* N66 and *B. velezensis* N54) are given in the supplementary material in Fig. S2.

For biological characterization and interpretation of these informative metabolite profiles described by explorative modelling: PCA and HCA results (Fig. 3), a supervised method namely OPLS-DA was applied (Fig. 4). The latter allows the identification of the metabolite features underlying the discrimination between classes or groups (Tugizimana et al., 2013). The computed and validated OPLS-DA models (CV-ANOVA, cross-validated analysis of variance, *p*-value <0.05) used in the current study were perfect binary classifiers (Fig. 4 A) and had no signs of possible overfitting, as indicated by cross-validation, and none of the permutated models (n = 100) performed better than the original models in separating classes (Fig. 4 B). For selection of 'variables', i.e. discriminating metabolite features with unique Rt-*m*/*z* values, OPLS-DA loadings S-plots (Fig. 4 C) were evaluated: this loading plot aids in identifying variables which differ between groups, i.e. the discriminating features. Variables that combine high model influence (covariation) with high reliability (correlation), i.e. variables at the far ends of the S-plot, are statistically relevant as potential discriminant variables to be selected (Tugizimana et al., 2013). To avoid variable selection bias, the variable importance in projection (VIP)-plots were generated (Fig. 4 D) and only the variables (from S-plots) with the VIP score exceeding 1.0 were retained. As mentioned in the experimental section, the statistically selected variables (from S-plots) were then annotated to metabolomics standards initiative (MSI, Sumner et al. 2007) level-2 and shown in Table 2 containing the metabolites upregulated during ISResilience against combined biotic and abiotic stress. Those for conditions of no-stress, ISTolerance and ISResistance are reported in supplementary material: Table S2 containing the metabolites upregulated during conditions of no-stress, Table S3 containing the metabolites upregulated during ISResistance against biotic stress (*F. pseudograminearum* crown rot), Table S4 containing the metabolites upregulated during ISTolerance against abiotic stress (drought).

3.2.3. Metabolomic reprogramming

3.2.3.1. Quantitative differences in metabolomic reprogramming

In order to compare the rhizobacterial isolates for quantitative capacity to induce a defense response against the different stress regimes, heatmaps were used to visualize the extent to which metabolites were upregulated and Venn-diagrams were used to visualize the number of metabolites that were upregulated (Fig. 5, Fig. 6 for combined biotic and abiotic stress; Figs. S3 and S4 for biotic stress and Figs. S5 and S6 for abiotic stress).

Table 2. Summary of metabolites significantly upregulated ($p < 0.05$) during ISResilience under conditions of combined biotic and abiotic stress (inoculated with *F. pseudograminearum* + drought stress) in rhizobacterial-treated *S. bicolor* seedlings *versus* those left naïve. Discriminating metabolites were identified based on OPLS-DA S-plots.

							Metabolite fold change (fc) and *p*-value of primed *versus* naïve *S. bicolor* seedlings					
							NAS-6G6		N66		N54	
	Metabolite	*m/z*[1]	RT[2] (min)	ESI[3] mode	Molecular formula	Biochemical function / MOA	fc	*p*	fc	*p*	fc	*p*
1	L-Leucine	335	8.00	Pos	$C_6H_{13}NO_2$	Amino acid	3.08	2.27×10^{-6}	2.21	2.83×10^{-6}	2.12	3.09×10^{-6}
2	N,N-Dihydroxy-L-tyrosine	234	8.11	Neg	$C_9H_{11}NO_5$	Amino acid	2.72	3.60×10^{-6}	3.14	2.20×10^{-10}	3.71	6.43×10^{-11}
3	L-Histidine	309	6.00	Pos	$C_6H_9N_3O_2$	Amino acid	4.64	3.97×10^{-4}	3.18	7.68×10^{-6}	3.70	8.28×10^{-4}
4	Riboflavin	437	9.07	Pos	$C_{17}H_{19}N_4O_6$	Antioxidant	–	–	2.55	1.74×10^{-5}	3.75	1.29×10^{-4}
5	Hydroxyproline[4]	343	4.05	Neg	$C_5H_9NO_3$	Antioxidant	–	–	–	–	–	–
6	Myo-inositol	249	3.57	Pos	$C_6H_{12}O_6$	Osmolyte	4.50	8.94×10^{-4}	6.86	1.22×10^{-7}	7.49	8.72×10^{-9}
7	N-Caffeoylputrescine	309	5.99	Pos	$C_{13}H_{18}N_2O_3$	Diamine	4.64	3.97×10^{-4}	3.18	7.68×10^{-6}	3.70	8.28×10^{-4}
8	Apigenin 7-O-neohesperidoside	623	7.34	Pos	$C_{27}H_{30}O_{14}$	Flavone / Flavonol	–	–	2.44	2.44×10^{-8}	–	–
9	Hesperetin 7-O-glucoside	532	6.11	Neg	$C_{22}H_{24}O_{11}$	Flavonoid	2.51	1.86×10^{-4}	2.24	5.40×10^{-7}	2.61	1.21×10^{-7}
10	Pentahydroxyflavanone	305	4.61	Pos	$C_{15}H_{12}O_7$	Flavonoid	–	–	7.82	2.41×10^{-8}	–	–
11	3,4-Epoxybutyl-alpha-D-glucopyranoside	335	4.96	Pos	$C_{10}H_{18}O_7$	Glycogen	2.13	3.82×10^{-3}	2.06	2.47×10^{-4}	2.70	9.13×10^{-5}
12	Heptaethylene glycol	349	1.69	Pos	$C_{14}H_{30}O_8$	Glycogen / Phytohormone	12.07	9.13×10^{-5}	40.10	1.35×10^{-8}	36.96	5.52×10^{-12}
13	Isopropylammelide	207	4.48	Neg	$C_6H_{10}N_4O_2$	Histidine	9.81	8.46×10^{-3}	17.02	2.19×10^{-11}	14.88	2.54×10^{-11}
14	(9Z,12Z,15Z)-Octadecatrienoic acid	317	3.66	Pos	$C_{18}H_{30}O_2$	Lipid	6.56	1.62×10^{-8}	4.68	6.76×10^{-14}	4.66	5.05×10^{-13}
15	L-Serine-phosphoethanolamine	301	3.46	Neg	$C_5H_{13}N_2O_6P$	Lipid	5.83	3.86×10^{-4}	36.08	4.26×10^{-5}	16.76	2.89×10^{-4}
16	(3Z,6Z)-Nonadienal	183	4.93	Pos	$C_9H_{14}O$	Lipid	–	–	146.05	1.26×10^{-10}	94.49	1.12×10^{-11}
17	3,5-Dimethoxyphenol	177	9.00	Pos	$C_8H_{10}O_3$	Phenylpropanoid	–	–	2.43	1.30×10^{-10}	3.13	1.12×10^{-11}

	Metabolite	*m/z*[1]	RT[2] (min)	ESI[3] mode	Molecular formula	Biochemical function / MOA	Metabolite fold change (fc) and *p*-value of primed *versus* naïve *S. bicolor* seedlings					
							NAS-6G6		N66		N54	
							fc	*p*	fc	*p*	fc	*p*
18	**Trans-beta-D-glucosyl-2-hydroxycinnamate**	**325**	**6.90**	**Neg**	**$C_{15}H_{18}O_8$**	**Phenylpropanoid**	2.67	4.27×10^{-6}	2.66	7.33×10^{-9}	2.05	4.51×10^{-4}
19	**Shikimate**	**195**	**5.59**	**Neg**	**$C_7H_{10}O_5$**	**Phenylpropanoid**	3.50	2.43×10^{-8}	3.08	3.67×10^{-8}	3.40	1.61×10^{-9}
20	**Trans-5-O-caffeoyl-D-quinate**	**561**	**6.09**	**Neg**	**$C_{16}H_{17}O_9$**	**Phenylpropanoid**	6.80	2.14×10^{-2}	9.47	1.56×10^{-2}	–	–
21	**Gibberellin A36**	**415**	**9.07**	**Pos**	**$C_{20}H_{26}O_6$**	**Phytohormone**	–	–	2.11	1.99×10^{-2}	2.06	3.75×10^{-3}
22	**(-)-Phenylalanine jasmonate conjugate**	**450**	**4.30**	**Pos**	**$C_{21}H_{29}NO_4$**	**Phytohormone**	6.00	6.33×10^{-3}	2.61	2.61×10^{-3}	2.90	4.83×10^{-6}
23	**Dihydrozeatin-9-N-glucoside-O-glucoside**	**584**	**1.74**	**Pos**	**$C_{22}H_{35}N_5O_{11}$**	**Phytohormone**	–	–	2.67	1.92×10^{-4}	–	–
24	**Thermozeaxanthin**	**948**	**14.12**	**Pos**	**$C_{51}H_{84}O_{12}$**	**Phytohormone**	–	–	2.90	2.90×10^{-2}	3.29	1.47×10^{-2}
25	**Gibberellin A36**	**407**	**8.94**	**Neg**	**$C_{20}H_{26}O_6$**	**Phytohormone**	4.07	4.74×10^{-7}	3.42	$2.90' \times 10^{-4}$	3.19	4.06×10^{-8}
26	**(±)-9,10-Dihydrojasmonic acid**	**475**	**8.00**	**Pos**	**$C_{18}H_{30}O_9$**	**Phytohormone**	4.77	1.82×10^{-5}	3.64	2.84×10^{-6}	4.34	7.63×10^{-6}
27	**3-Oxopropionyl-CoA[5]**	**853**	**1.96**	**Neg**	**$C_{24}H_{38}N_7O_{18}P_3S$**	**Propanoate**	–	–	–	–	–	–
28	**Dimethylbenzimidazole**	**205**	**5.59**	**Pos**	**$C_9H_{10}N_2$**	**Antioxidant**	3.10	6.13×10^{-5}	2.19	1.79×10^{-5}	2.53	1.66×10^{-6}
29	**Demethylphylloquinol**	**557**	**11.07**	**Pos**	**$C_{30}H_{46}O_2$**	**Antioxidant**	–	–	2.06	5.33×10^{-5}	–	–
30	**Ubiquinone**	**357**	**4.58**	**Pos**	**$C_{14}H_{18}O_4$**	**Antioxidant**	34.33	1.04×10^{-8}	–	–	16.39	9.54×10^{-14}

[1]Mass divided by charge (*m*/*z*).
[2]Retention time (RT).
[3]Electrospray ionization (ESI).
[4]Hydroxyproline levels, although not altered under combined stresses, were significantly altered during the other stress regimes tested as shown in Table S2 to S4.
[5]3-Oxopropionyl-CoA levels, although not altered under combined stresses, were significantly altered during biotic and abiotic stress as shown in Table S3 and S4.

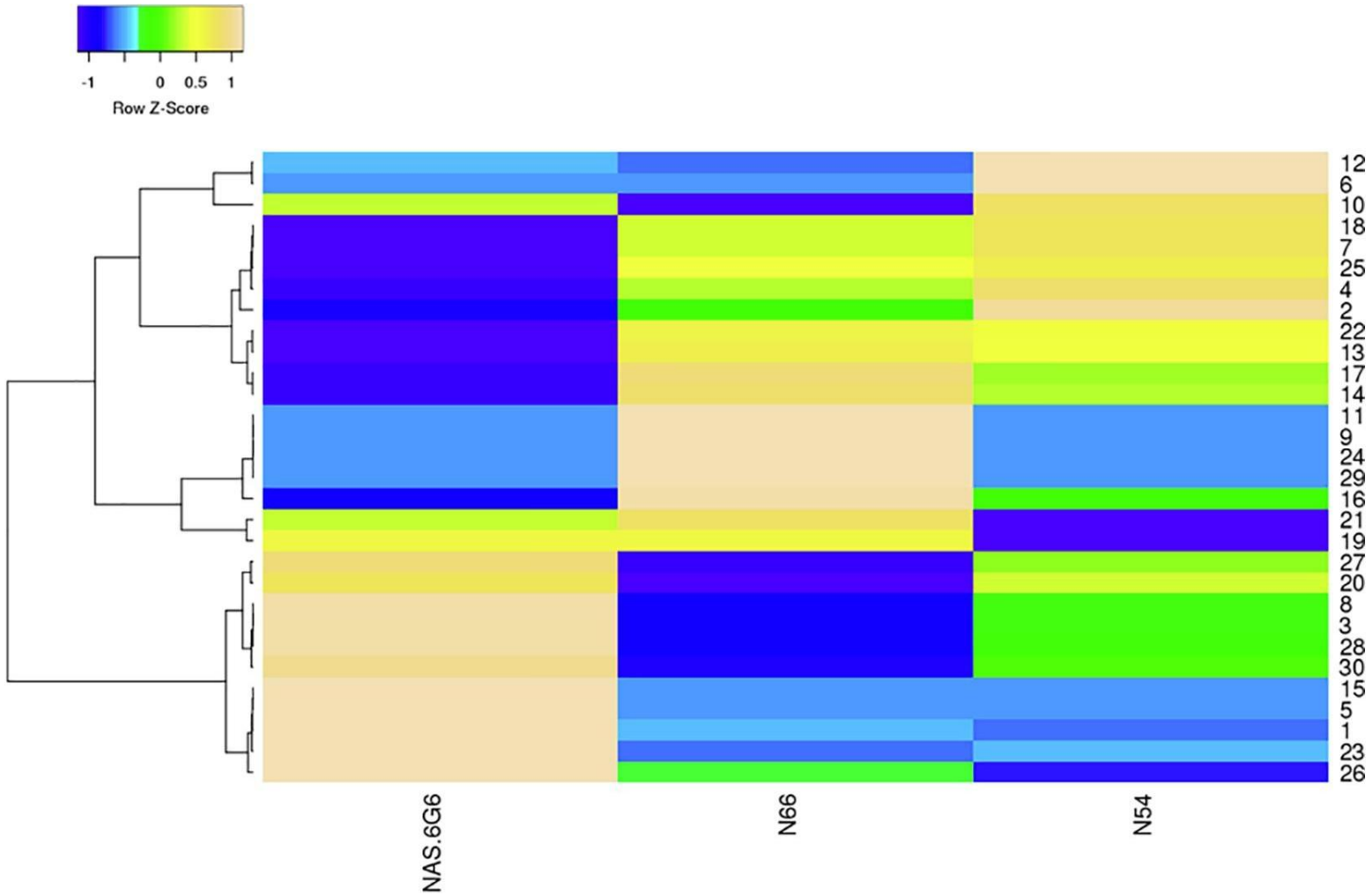

Fig. 5. Heatmap comparing the fold change (primed *versus* naïve) of the top 30 metabolites significantly upregulated in *S. bicolor* seedlings primed with rhizobacterial isolates NAS-6G6, N66 and N54 in response to combined biotic and abiotic stress (inoculation with *F. pseudograminearum* and drought). The number to the right corresponds to the metabolite number in Table 2.

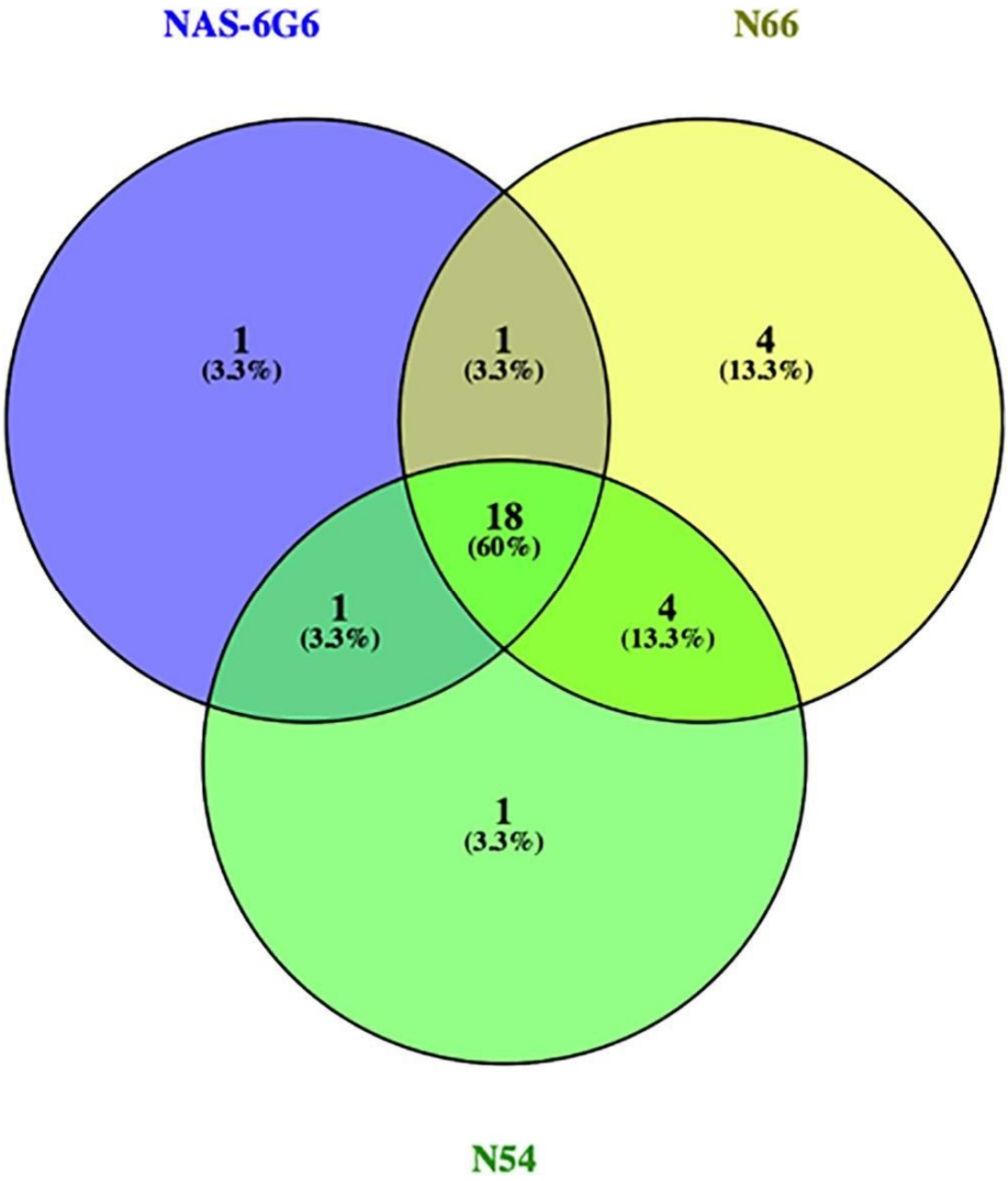

Fig. 6. Venn diagram comparing the number of metabolites, of the top 30 metabolites significantly upregulated in *S. bicolor* seedlings primed with rhizobacterial isolates NAS-6G6, N66 and N54 in response to combined biotic and abiotic stress (inoculation with *F. pseudograminearum* and drought).

3.2.3.2. Qualitative differences in metabolomic reprogramming

To measure the qualitative capacity of each rhizobacterial strain to induce a defense response against the different stress regimes, pathway analysis was done using MetPa. Metabolic pathways upregulated by *B. velezensis* N54 under each of the stress regimes (none, abiotic, biotic and combined stresses) are shown in Fig. 7A to D respectively. Similarly those for *Pa. alvei* and *Ps. taiwanensis* are supplied under supplementary material (Figs. S7 and S8). Under each of the stress regimes tested, different combinations of metabolic pathways (MetPA-computed metabolic pathways) were upregulated, of which the impact is indicated by the radius and the *p*-value is indicated by the colour of the nodes.

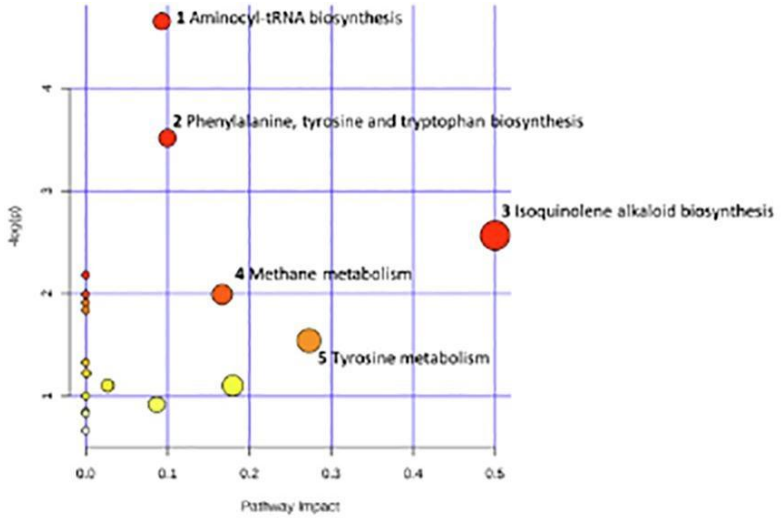

(A) N54 + no stress

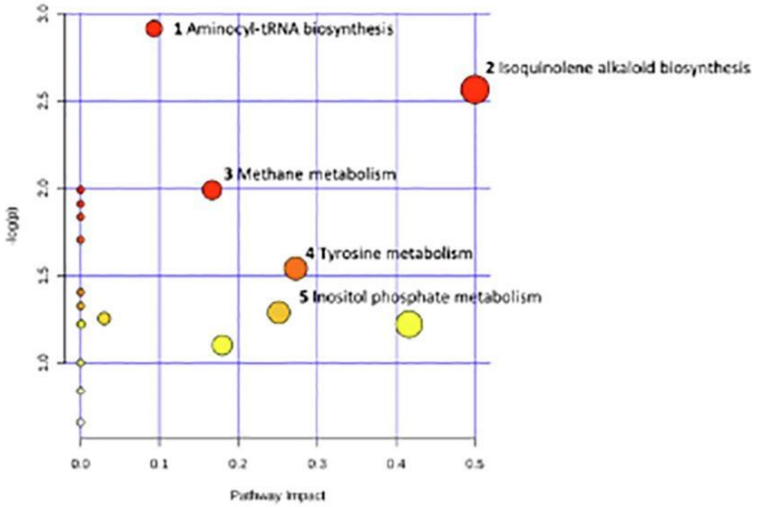

(B) N54 + abiotic stress

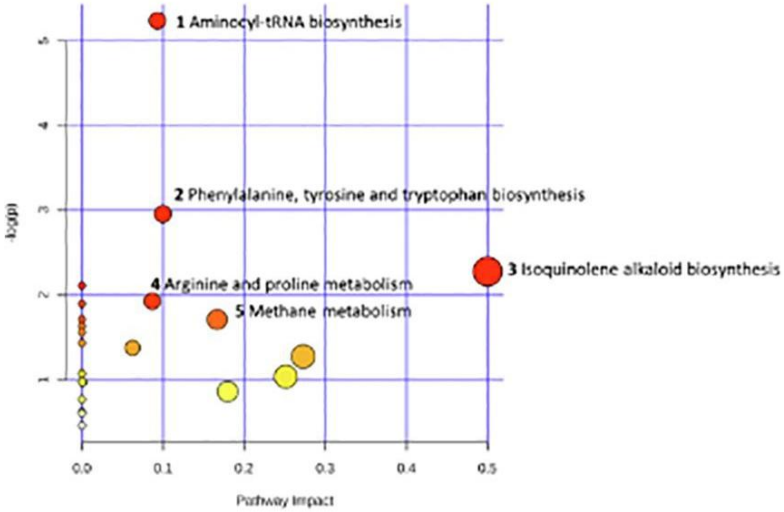

(C) N54 + biotic stress

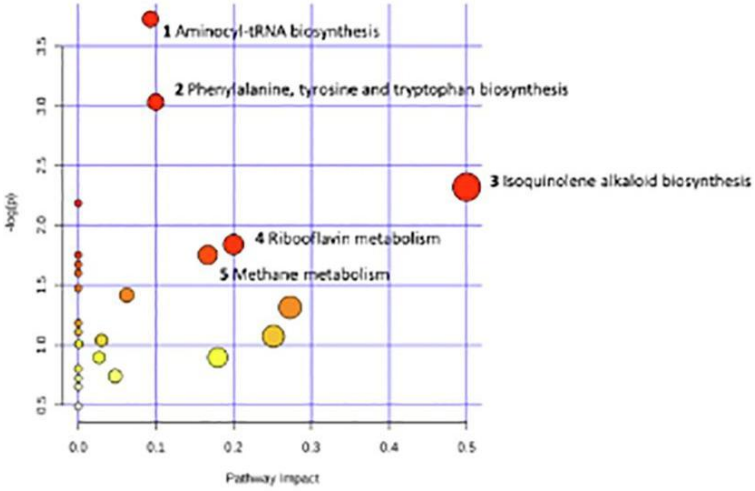

(D) N54 + combined stress

Fig. 7. Summary of pathway analysis with MetPA of the effect of priming *S. bicolor* with rhizobacterial isolate **N54** under conditions of (A) no stress, (B) drought, (C) inoculation with *F. pseudograminearum* and (D) combined stresses: Representation of all MetPA-computed metabolic pathways displayed per their significance or pathway impact. The graph, "metabolome view" contains all the matched pathways (the metabolome) arranged by *p*-values (pathway enrichment analysis) on *y*-axis, and the pathway impact values (pathway topology analysis) on *x*-axis. The node colour is based on the *p*-value and the node radius is defined by the pathway impact values. The latter is the cumulative percentage from the matched metabolite nodes. Thus, the graph indicates pathways with high impact. Only pathways of high impact (red) are labelled.

4. Discussion

In this study, we report the capacity of rhizobacteria that induced effective defence responses in plants as determined by both quantitative and qualitative properties of the induced metabolic reprogramming. The quantitative properties consist of the number of, level to which and speed by which defence metabolites are upregulated (Conrath et al., 2015, Carlson et al., 2019), whereas the qualitative properties relate to the unique capacity of each metabolite in mitigating the effect of the specific stress at hand (Carlson et al., 2019, Tugizimana et al., 2019, Carlson et al., 2020). When both the qualitative and quantitative aspects of the metabolic reprogramming observed in this study are considered, unique differences were observed.

Under conditions of no-stress, during the priming phase, the rhizobacterial isolates differed in their capacity to reprogram *S. bicolor*. Priming preconditions the plant for enhanced defense and an elevation of amino acid levels, which are known to serve as building blocks for secondary metabolism, are usually noticed (Carlson et al., 2019). A similar response was found here where priming with *Pa. alvei* NAS-6G6 resulted in the differential upregulation of arginine and proline metabolism, *Ps. taiwanensis* N66 that of histidine metabolism and *B. velezensis* N54 that of tyrosine metabolism. The unique response to priming upon treatment with each of the rhizobacterial strains, was reciprocated in the metabolic reprogramming observed in response to biotic, abiotic and combined stresses.

Under conditions of biotic stress, *B. velezensis* N54 upregulated arginine and proline metabolism, *Pa. alvei* NAS-6G6 upregulated riboflavin metabolism and *Ps. taiwanensis* N66 upregulated tyrosine metabolism. *Pa. alvei* NAS-6G6 was however superior in the number and level to which metabolites were upregulated during biotic stress. Under conditions of abiotic stress, *B. velezensis* N54 upregulated tyrosine- and inositol phosphate metabolism and *Ps. taiwanensis* N66 upregulated riboflavin metabolism. *Ps. taiwanensis* N66 was however superior in the level to which metabolites were upregulated during abiotic stress. Under conditions of combined stress, both *B. velezensis* N54 and *Ps. taiwanensis* N66 were responsible for the upregulation of riboflavin metabolism and *Pa. alvei* NAS-6G6 that of glutathione metabolism. *B. velezensis* N54 was however superior in the level to which metabolites were upregulated during combined stress. In addition to this, it should be noted that treatment with *Pa. alvei* NAS-6G6 and *B. velezensis* N54 resulted in the upregulation of unique combinations of metabolic pathways under combined stress. This points to possible synergistic interactions between pathways.

The unique role of the regulatory networks and the metabolites involved in protecting *S. bicolor* against individually occurring biotic and abiotic stress, are potential role players in alleviating stress under combined biotic and abiotic stress. From the data presented here, it is clear that a great deal of overlap exist in the biotic, abiotic and combined stress response. This was evidenced by the upregulation of amino acids, signaling hormones, antioxidants and phytoalexins under conditions of individually occurring and combined stresses. Although a great deal of overlap exist, lately evidence for non-additive effects under conditions of combined biotic and abiotic stress have implicated the role of crosstalk (Pieterse, 2001, Pieterse et al., 2001, Fujita et al., 2006, Koornneef et al., 2008, Oktem et al., 2008, Moubayidin et al., 2009, Kissoudis et al., 2014, Yue et al., 2016, Rejeb et al., 2018). These signaling-interactions during crosstalk can either be synergistic or antagonistic, supporting the conflicting results obtained in earlier studies (Koornneef et al., 2008).

Many examples exist of metabolites that act as signaling molecules under conditions of combined biotic and abiotic stress. These metabolites usually interact with the signaling hormones during crosstalk. The antioxidant glutathione for example plays an important role in controlling redox levels under conditions of oxidative stress (González-Bosch, 2018) and the osmolyte myo-inositol for example, plays an important role in regulating salicylic acid (SA)-dependant programmed cell death under oxidative stress conditions (Noctor and Chaouch, 2010). The regulation of SA was directly linked to the levels of myo-inositol in plant tissues. Another such metabolite, known for its role in crosstalk, is the vitamin and antioxidant riboflavin. Riboflavin plays and important role in catalyzing the production and metabolism of reactive oxygen species (Zhang et al., 2009, Azami-Sardooei et al., 2010, Boubakri et al., 2016) and is also a precursor for dimethylbenzimidazole, known to have fungicidal properties (Renz and Weyhenmeyer, 1972).

5. Conclusion

All three the rhizobacterial isolates tested were able to protect *S. bicolor* seedlings to some degree against biotic, abiotic and combined biotic and abiotic stress. This protection was a direct result of rhizobacteria-induced priming giving rise to a quicker and enhanced metabolic defence response to stress. These rhizobacterial isolates however differed significantly in their capacity to offer such protection. This capacity was directly related to both the quantitative and qualitative properties of the metabolic reprogramming observed in *S. bicolor*, not only during the post-challenge primed state, but also during the priming phase.

Pa. alvei NAS-6G6 possessed the unique capacity to induce protection against all three stress regimes tested, both in the number and extent to which defence metabolites were upregulated in *S. bicolor* plants. This was corroborated by the analysis of the metabolic pathways involved and consisted of riboflavin metabolism under biotic and abiotic stress and glutathione metabolism under combined biotic and abiotic stress. Similarly, evidence for the role of riboflavin metabolism in the *Ps. taiwanensis* N66-induced systemic tolerance against drought stress and in isolate *B. velezensis* N54-induced systemic resilience are provided here.

In addition to a novel understanding of rhizobacteria-induced systemic resilience in *S. bicolor*, this report also offers evidence of synergistic interactions between the regulatory pathways involved in the metabolic response observed in rhizobacteria-primed *S. bicolor* seedlings in response to combined stresses. Such synergistic interaction in *S. bicolor* metabolism were found for treatment with *Pa. alvei* NAS-6G6 and *B. velezensis* N54. This was demonstrated by the lack of additive effects when completely different sets of metabolic pathways were upregulated in *S. bicolor* under conditions of combined stress compared to those metabolic pathways upregulated under individually occurring biotic and abiotic stress conditions. These findings provide putative evidence for the role of crosstalk in the combined biotic and abiotic stress response.

6. Data availability

The metabolomics data and the raw data from the screening- and greenhouse trials have been deposited to the EMBL-EBI MetaboLights database (DOI: 10.1093/nar/gkz1019, PMID:31691833) with the identifier MTBLS1646 (Haug et al., 2013). The complete dataset can be accessed here https://www.ebi.ac.uk/metabolights/MTBLS1646.

Author contributions

Nico Labuschagne and René Carlson conceived and guided the project. Nico Labuschagne, Ahmed Idris Hassen, Ian A. Dubery and Fidele Tugizimana guided and coordinated the research. René Carlson performed the experimental work. Paul A. Steenkamp did the instrumental analyses of samples. René Carlson performed the molecular work and was guided by Ahmed Idris Hassen. René Carlson and Fidele Tugizimana analysed the data and performed the chemometric analyses. All authors contributed to writing and editing of the manuscript. All authors have read and approved the final version of the manuscript.

Declaration of Competing Interest

The authors declare that they have no known competing financial interests or personal relationships that could have appeared to influence the work reported in this paper.

Acknowledgement of financial and other support

The National Research Foundation (NRF) of South Africa is duly acknowledged for partially supporting this work through grant holder's bursary to René Carlson, grant number 98863 (ref. no. CSUR150624120744). Due acknowledgement also goes to the University of Pretoria who rendered the fellowship towards her PhD study.

References

Akinsanmi, O.A., Mitter, V., Simpfendorfer, S., Backhouse, D., Chakraborty, S., 2004. Identity and pathogenicity of *Fusarium* spp. isolated from wheat fields in Queensland and northern New South Wales. Aust. J. Agric. Res. 55, 97–107. https://doi.org/10.1071/AR03090.

Azami-Sardooei, Z., França, S.C., De Vleesschauwer, D., Höfte, M., 2010. Riboflavin induces resistance against *Botrytis* cinerea in bean, but not in tomato, by priming for a hydrogen peroxide-fueled resistance response. Physiol. Mol. Plant Pathol. 75 (1-2), 23–29. https://doi.org/10.1016/j.pmpp.2010.08.001.

Bai, G.-H., Shaner, G., 1996. Variation in *Fusarium graminearum* and cultivar resistance to Wheat Scab. Plant Dis. 80, 975–979. https://doi.org/10.1094/PD-80-0975.

Boubakri, H., Gargouri, M., Mliki, A., Brini, F., Chong, J., Jbara, M., 2016. Vitamins for enhancing plant resistance. Planta 244, 529–543. https://doi.org/10.1007/s00425-016-2552-0.

Brown, M., Dunn, W.B., Dobson, P., Patel, Y., Winder, C.L., Francis-Mcintyre, S., Begley, P., Carroll, K., Broadhurst, D., Tseng, A., Swainston, N., Spasic, I., Goodacre, R., Kell, D.B., 2009. Mass spectrometry tools and metabolite-specific databases for molecular identification in metabolomics. Analyst 134, 1322–1332. https://doi.org/10.1039/b901179j.

Brown, M., Wedge, D.C., Goodacre, R., Kell, D.B., Baker, P.N., Kenny, L.C., Mamas, M.A., Neyses, L., Dunn, W.B., 2011. Automated workflows for accurate mass-based putative metabolite identification in LC/MS-derived metabolomic datasets. Bioinformatics 27,1108–1112. https://doi.org/10.1093/bioinformatics/btr079.

Carlson, R., Tugizimana, F., Steenkamp, P.A., Dubery, I.A., Hassen, A.I., Labuschagne, N., 2020. Rhizobacteria-induced systemic tolerance against drought stress in *Sorghum bicolor* (L.) Moench. Microbiol. Res. 232, 126388. https://doi.org/10.1016/j.micres.2019.126388.

Carlson, R., Tugizimana, F., Steenkamp, P.A., Dubery, I.A., Labuschagne, N., 2019. Differential metabolic reprogramming in *Paenibacillus alvei*-primed *Sorghum bicolor* seedlings in response to *Fusarium pseudograminearum* infection. Metabolites 9, 150. https://doi.org/10.3390/metabo9070150.

Choudhary, D.K., Kasotia, A., Jain, S., 2016. Bacterial-mediated tolerance and resistance to plants under abiotic and biotic stresses. J. Plant Growth Regul. 35, 276–300. https://doi.org/10.1007/s00344-015-9521-x.

Conrath, U., Beckers, G.J.M., Langenbach, C.J.G., Jaskiewicz, M.R., 2015. Priming for enhanced defense. Annu. Rev. Phytopathol. 53, 97–119. https://doi.org/10.1146/annurev-phyto-080614-120132.

Dykes, L., Rooney, L.W., 2006. Sorghum and millet phenols and antioxidants. J. Cereal Sci. 44, 236–251. https://doi.org/10.1016/j.jcs.2006.06.007.

Embley, M., Smida, J., Stackebrand, E.T., 1988. Reverse transcriptase sequencing of 16Sribosomal RNA from *Faenia rectivirgula, Pseudonocardia thermophila* and *Saecharopolyspora hirsuta*. J. Gen. Microbiol. 134, 961–966.

Fong, Y.K., Anuar, S., Lim, H.P., Tham, F.Y., Sanderson, F.R., 2000. A modified filter paper technique for long-term preservation of some fungal cultures. Mycologist 14,127–130. https://doi.org/10.1016/S0269-915X(00)80090-7.

Fujita,M., Fujita, Y., Noutoshi, Y., Takahashi, F., Narusaka, Y., Yamaguchi-Schinozaki, K., Shinozaki, K., 2006. Crosstalk between abiotic and biotic stress responses: a current view from the points of convergence in the stress signaling networks. Curr. Opin.Plant Biol. 9, 436–442. https://doi.org/10.1016/j.pbi.2006.05.014.

González-Bosch, C., 2018. Priming plant resistance by activation of redox-sensitive genes. Free Radic. Biol. Med. 122, 171–180. https://doi.org/10.1016/j.freeradbiomed.2017.12.028.

Harish, S., Kavino, M., Kumar, N., Saravanakumar, D., Soorianathasundaram, K., Samiyappan, R., 2008. Biohardening with plant growth promoting rhizosphere and endophytic bacteria induces systemic resistance against banana bunchy top virus. Appl. Soil Ecol. 39, 187–200. https://doi.org/10.1016/j.apsoil.2007.12.006.

Hassen, A.I., 2007. Efficacy of Rhizobacteria for Growth Promotion and Biocontrol of *Pythium ultimum* and *Fusarium oxysporumon* sorghum in Ethiopia and South Africa. Ph.D. thesis. University of Pretoria, Pretoria, South Africa.

Kang, S-M., Khan, A.L., Waqas, M., You, Y-H., Hamayun, M., Joo, G-J., Shahzad, R., Choi, K-S., Lee, I.-J., 2015. European Journal of Soil Biology Gibberellin-producing *Serratia nematodiphila* PEJ1011 ameliorates low temperature stress in *Capsicum annuum* L.Eur. J. Soil Biol. 1–9. https://doi.org/10.1016/j.ejsobi.2015.02.005.

Kissoudis, C., Van de Wiel, C., Visser, R.G.F., Van der Linden, G., 2014. Enhancing cropresilience to combined abiotic and biotic stress through the dissection of physiolo-gical and molecular crosstalk. Front. Plant Sci. 5, 1–25. https://doi.org/10.3389/fpls.2014.00207.

Koornneef, A., Pieterse, C.M.J., Pieterse, M.J., 2008. Cross talk in defense signaling. Plant Phys. 146, 839–844. https://doi.org/10.1104/pp.107.112029.

Kumar, S., Stecher, G., Li, M., Knyaz, C., Tamura, K., 2018. MEGA X: Molecular evolutionary genetics analysis across computing platforms. Mol. Biol. Evol. 35, 1547–1549. https://doi.org/10.1093/molbev/msy096.

Lane, D.J., 1991. 16S/23S rRNA sequencing. In: Stackbrandt, E., Goodfellow, M. (Eds.), Nucleic Acid Techniques in Bacterial Systematics. John Wiley and Sons Ltd,Cambridge, UK, pp. 115–175.

Li, X., Liu, C., Chakraborty, S., Manners, J.M., Kazan, K., 2008. A simple method for the assessment of crown rot disease severity in wheat seedlings inoculated with *Fusarium pseudograminearum*. J. Phytopath. 156, 751–754. https://doi.org/10.1111/j.1439-0434.2008.01425.x.

Lucas, J.A., García-Cristobal, J., Bonilla, A., Ramos, B., Gutierrez-Mañero, J., 2014. Beneficial rhizobacteria from rice rhizosphere confers high protection against biotic and abiotic stress inducing systemic resistance in rice seedlings. Plant Physiol. Bioch.82, 44–53. https://doi.org/10.1016/j.plaphy.2014.05.007.

Mitter, V., Francl, L.J., Ali, S., Simpfendorfer, S., Chakraborty, S., 2006. Ascosporic and conidial inoculum of *Gibberella zeae* play different roles in Fusarium head blight and crown rot of wheat in Australia and the USA. Australas. Plant Path. 35, 441–452. https://doi.org/10.1071/AP06046.

Moubayidin,L., Di Mambro, R., Sabatini, S., 2009. Cytokinin–auxin crosstalk. Trends Plant Sci. 14, 557–562. https://doi.org/10.1016/j.tplants.2009.06.010.

Naseem, H., Bano, A., 2014. Role of plant growth-promoting rhizobacteria and their exopolysaccharide in drought tolerance of maize. J. Plant Interact..9, 689–701. https://doi.org/10.1080/17429145.2014.902125.

Ngumbi, E., Kloepper, J., 2016. Bacterial-mediated drought tolerance: current and future prospects. Appl. Soil Ecol. 105, 109–125. https://doi.org/10.1016/j.apsoil.2016.04.009.

Noctor, G., Chaouch, S., 2010. Myo-inositol abolishes salicylic acid-dependent cell death and pathogen defence responses triggered by peroxisomal hydrogen peroxide. New Phytol. 188, 711–718. https://doi.org/10.1111/j.1469-8137.2010.03453.x.

Oktem, H.A., Eyidogen, F., Selcuk, F., Oz, M.T., Da Silva, J.A.T., Yücel, M., 2008. Revealing response of plants to biotic and abiotic stresses with microarray technology. Genes Genomes Genomics 2, 14–48.

Parnell, J.J., Berka, R., Young, H.A., Sturino, J.M., Kang, Y., Barnhart, D.M., DiLeo, M.V., 2016. From the lab to the farm: an industrial perspective of plant beneficial micro-organisms. Front. Plant Sci. 7, 1–12. https://doi.org/10.3389/fpls.2016.01110.

Pieterse, C.M.J., 2001. Rhizobacteria-mediated induced systemic resistance: triggering, signaling and expression. Eur. J. Plant Pathol. 107, 51–61. https://doi.org/10.1023/A:1008747926678.

Pieterse, C.M.J., Ton, J., Van Loon, L.C., 2001. Cross-talk between plant defence signalling pathways: boost or burden? AgBiotechNet 3, 1–8.

Rejeb, I.B., Pastor, V., Gravel, V., Mauch-Mani, B., 2018. Impact of β-aminobutyric acid on induced resistance in tomato plants exposed to a combination of abiotic and biotic stress. J. Agric. Sci. Bot. 2.

Renz, P., Weyhenmeyer, R., 1972. Biosynthesis of 5,6-dimethylbenzimidazole from riboflavin. FEBS Lett. 22, 124–126. https://doi.org/10.1016/0014-5793(72)80236-9.

Saitou, N., Nei, M., 1987. The neighbor-joining method: a new method for reconstructing phylogenetic trees. Mol. Biol. Evol. 4, 406–425. https://doi.org/10.1093/oxfordjournals.molbev.a040454.

Seelig, H.-D., Hoehn, A., Stodieck, L.S., Klaus, D.M., Adams, W.W., Emery, W.J., 2008.The assessment of leaf water content using leaf reflectance ratios in the visible, near-, and short-wave-infrared. Int. J. Remote Sens. 29, 3701–3713. https://doi.org/10.1080/01431160701772500.

Sumner, L.W., Amberg, A., Barrett, D., Beale, M.H., Beger, R., Daykin, C.A., Fan, T.-W.-M., Fiehn, O., Goodacre, R., Griffin, J.L., Hankemeier, T., Hardy, N., Harnly, J., Higashi,R., Kopka, J., Lane, A.N., Lindon, J.C., Marriott, P., Nicholls, A.W., Reily, M.D.,Thaden, J.J., Viant, M.R., 2007. Proposed minimum reporting standards for chemical analysis Chemical Analysis Working Group (CAWG) Metabolomics Standards Initiative (MSI). Metabolomics 3, 211–221. https://doi.org/10.1007/s11306-007-0082-2.

Tamura,K., Nei, M., Kumar, S., 2004. Prospects for inferring very large phylogenies by using the neighbor-joining method. Proc. Natl. Acad. Sci. 101, 11030–11035. https://doi.org/10.1073/pnas.0404206101.

Timmusk, S., Wagner, E.G., 1999. The plant-growth-promoting rhizobacterium *Paenibacillus polymyxa* induces changes in *Arabidopsis thaliana* gene expression: a possible connection between biotic and abiotic stress responses. Mol. Plant Microbe In. 12, 951–959. https://doi.org/10.1094/MPMI.1999.12.11.951.

Tugizimana, F., Piater, L., Dubery, I., 2013. Plant metabolomics: a new frontier in phytochemical analysis. S. Afr. J. Sci. 109, 1–11. https://doi.org/10.1590/sajs.2013/20120005.

Tugizimana, F., Djami-Tchatchou, A., Steenkamp, P.A., Piater, L.A., Dubery, I.A., 2019. Metabolomic analysis of defense-related reprogramming in Sorghum bicolorin response to

Colletotrichum sublineolum infection reveals a functional metabolic web of phenylpropanoid and flavonoid pathways. Front. Plant Sci. 9, 1–20. https://doi.org/10.3389/fpls.2018.01840.

Van Wyk, P.S., Scholtz, D.S., 1995. A selective medium for the isolation of *Fusarium* spp. from soil debris. Phytophylactica 18, 67–69.

Walters, D.R., 2009. Are plants in the field already induced? Implications for practical disease control. Crop Protect. 28, 459–465. https://doi.org/10.1016/j.cropro.2009.01.009.

Walters, D.R., Fountaine, J.M., 2009. Practical application of induced resistance to plant diseases: an appraisal of effectiveness under field conditions. J. Agric. Sci..147, 523. https://doi.org/10.1017/S0021859609008806.

Xi, K., Turkington, T.K., Chen, M.H., 2008. Systemic stem infection by *Fusarium* species in barley and wheat. Can. J. Plant Pathol..30, 588–594. https://doi.org/10.1080/07060660809507559.

Xia, J., Sinelnikov, I., Han, B., Wishart, D.S., 2015. MetaboAnalyst 3.0 - making metabolomics more meaningful. Nucl. Acids Res. 43, 251–257. https://doi.org/10.1093/nar/gkv380.

Yang, J., Kloepper, J.W., Ryu, C.M., 2009. Rhizosphere bacteria help plants tolerate abiotic stress. Trends Plant Sci. 14, 1–4. https://doi.org/10.1080/07060660809507559.

Yue, X., Li, X.G., Gao, X.-Q., Zhao, X.Y., Zhou, C., 2016. The *Arabidopsis* phytohormone crosstalk network involves a consecutive metabolic route and circular control units of transcription factors that regulate enzyme-encoding genes. BMC Syst. Biol. 10, 87. https://doi.org/10.1186/s12918-016-0333-9.

Zhang,S., Yang, X., Sun, M., Sun, F., Deng, S., Dong, H., 2009. Riboflavin-induced priming for pathogen defense in *Arabidopsis thaliana*. J. Integr. Plant Biol. 51,167–174. https://doi.org/10.1111/j.1744-7909.2008.00763.x.

Zhang, Z., Schwartz, S., Wagner, L., Miller, W., 2000. A greedy algorithm for aligning DNA sequences. J. Comput. Biol..7, 203–214. https://doi.org/10.1089/10665270050081478.